

REPORT DOCUMENTATION PAGE

Form Approved OMB No. 0704-0188

Public reporting burden for this collection of information is estimated to average 1 hour per response, including the time for reviewing instructions, searching existing data sources, gathering and maintaining the data needed, and completing and reviewing the collection of information. Send comments regarding this burden estimate or any other aspect of this collection of information, including suggestions for reducing the burden, to Department of Defense, Washington Headquarters Services, Directorate for Information Operations and Reports (0704-0188), 1215 Jefferson Davis Highway, Suite 1204, Arlington, VA 22202-4302. Respondents should be aware that notwithstanding any other provision of law, no person shall be subject to any penalty for failing to comply with a collection of information if it does not display a currently valid OMB control number.

PLEASE DO NOT RETURN YOUR FORM TO THE ABOVE ADDRESS.

| | | |
|--|---------------------------------------|---|
| 1. REPORT DATE (DD-MM-YYYY) 22-09-2008 | 2. REPORT TYPE Final Report | 3. DATES COVERED (From – To) 1 April 2007 - 01-Apr-08 |
|--|---------------------------------------|---|

| | |
|---|--|
| 4. TITLE AND SUBTITLE Self-Organization of Cobalt Silicide Nanostructures into 2D Patterns on Vicinal Si Surfaces | 5a. CONTRACT NUMBER FA8655-07-1-3016 |
| | 5b. GRANT NUMBER |
| | 5c. PROGRAM ELEMENT NUMBER |

| | |
|--|-----------------------------|
| 6. AUTHOR(S) Dr. Ilan Goldfarb | 5d. PROJECT NUMBER |
| | 5d. TASK NUMBER |
| | 5e. WORK UNIT NUMBER |

| | |
|--|--|
| 7. PERFORMING ORGANIZATION NAME(S) AND ADDRESS(ES) Tel Aviv University Haim Levanon Ramat Aviv, Tel Aviv 69978 Israel | 8. PERFORMING ORGANIZATION REPORT NUMBER N/A |
|--|--|

| | |
|---|--|
| 9. SPONSORING/MONITORING AGENCY NAME(S) AND ADDRESS(ES) EOARD Unit 4515 BOX 14 APO AE 09421 | 10. SPONSOR/MONITOR'S ACRONYM(S) |
| | 11. SPONSOR/MONITOR'S REPORT NUMBER(S) Grant 07-3016 |

12. DISTRIBUTION/AVAILABILITY STATEMENT
Approved for public release; distribution is unlimited.

13. SUPPLEMENTARY NOTES

14. ABSTRACT

This report results from a contract tasking Tel Aviv University as follows: To achieve this goal, the work will be divided into two principle parts: (a) self-organization of stepped substrates, and (b) ordered nanocrystal growth. In the first part, the experiments will be aimed at achieving full control over the substrate step characteristics, e.g. terrace width and step-bunch height, by varying the degree of wafer miscut and high-temperature flash parameters (temperature, duration, and direction of the heating current relative to step orientation). The result of this stage will be variously spaced periodic step-structures. In the second part, Co and/or Ti will be deposited onto such 'templates', reacted with Si to form silicide dots, and their tendency for 2D ordering will be studied as a function of substrate periodicity and silicide nucleation and growth parameters.

15. SUBJECT TERMS
EOARD, Nanostructures

| | | | | | |
|--|------------------------------|-------------------------------|---|--------------------------------------|---|
| 16. SECURITY CLASSIFICATION OF: | | | 17. LIMITATION OF ABSTRACT UL | 18. NUMBER OF PAGES 23 | 19a. NAME OF RESPONSIBLE PERSON WYNN SANDERS, Maj, USAF |
| a. REPORT UNCLAS | b. ABSTRACT UNCLAS | c. THIS PAGE UNCLAS | | | 19b. TELEPHONE NUMBER (Include area code) +44 (0)1895 616 007 |

Investigation into Self-Organizational Tendencies of Cobalt- and Titanium-Silicide Nanostructures on Si Surfaces

Grant No.# 05614141

Final Report

submitted to European Office of Aerospace Research and Development (EOARD)

by Ilan Goldfarb

Table of Contents

| | |
|--|-----------|
| 1. List of Figures | 2 |
| 2. Summary | 3 |
| 3. Introduction | 4 |
| 4. Methods, Assumptions, and Procedures | 6 |
| 5. Results and Discussion | 11 |
| 6. Conclusions | 17 |
| 7. References | 18 |
| 8. List of Symbols, Abbreviations, and Acronyms | 22 |

1. *List of Figures*

Figure 1: CoSi₂ nanocrystals self-ordered on the vicinal Si(111) step-bunches.

Figure 2: Initial stages of the Co/Si(111)-(7×7) nucleation.

Figure 3: Formation of the precursor 2D CoSi₂ nanoplatelets (left), preceding the formation of fully grown 3D rounded nanocrystals self-ordered on the vicinal Si(111) step-bunches (right).

Figure 4: Self-organization of the SPE-grown CoSi₂ nanocrystals by stabilization at the vicinal Si(111) step-bunches.

Figure 5: SPE-grown CoSi₂ nanocrystals self-ordered on the vicinal Si(111) step-bunches (left), to compare with disordered RDE-grown CoSi₂ nanocrystals on the same vicinal Si(111) surface (right).

Figure 6: Evolution of disordered 2D CoSi₂ nanoislands, SPE-grown on a vicinal Si(111) surface at a higher Co coverage.

Figure 7: Disordered 3D TiSi₂ nanocrystals, SPE-grown on a vicinal Si(111) surface at a higher Ti coverage.

Figure 8: Evolution of the SPE- TiSi₂ nanocrystals, grown on a vicinal Si(111) surface with higher Ti coverage, as a function of annealing temperature.

Figure 9: Evolution of the SPE- TiSi₂ nanocrystals, grown on a *singular* Si(111) surface, as a function of annealing temperature.

Figure 10: SPE-CoSi₂ nanocrystals, grown on a *singular* Si(111) surface, after a 650°C annealing.

2. *Summary*

This research targets metal (mainly Co, but also Ti) silicide nanostructure formation and ordering by epitaxial self-assembly and self-organization. The research, and this grant application, were triggered by scanning tunneling microscopy observation of CoSi_2 nanostructures self-organized on the step-bunches of the vicinal Si(111) surfaces during solid-phase epitaxial growth, namely room-temperature deposition of Co followed by elevated temperature annealing treatments. The experimental results obtained between the time of application and its successful outcome, i.e., actual receipt of the grant funds, provided the clues for the possible mechanisms of self-organization, implied superiority of solid-phase epitaxy over the reactive deposition one, and were published in two journals, *Nanotechnology* and in press in *Journal of Nanoscience and Nanotechnology*. In parallel, the work aimed at mastering control over the mean terrace width and step-bunch height of the vicinal substrates with a given miscut angle - essential for the type of self-organization demonstrated - continued.

However, it was also noted that the mere use of solid-phase epitaxy did not guaranty by itself a successful self-organization, emphasizing the importance of additional parameters, most notably the initial metal coverage. Hence, the majority of efforts since the receipt of this grant were directed at exploration of the effect of coverage of the both Co and Ti. These studies have so far been indicative of the utmost importance of the coverage, more specifically it appears that preferential step-bunch decoration by the silicide nanocrystals, with no nanostructure nucleation in the midst of terraces, is only possible at a low initial metal coverage. Higher Co coverage has lead to only a minor step-bunch nucleation, with the vast majority of the CoSi_2 material contained in fractal two-dimensional terrace-islands, growing by ripening and coalescence and striving to cover the entire Si(111) substrate surface by a continues film (i.e., opposite to the desired effect). In the case of Ti, although two-dimensional islands did not form (most likely due to a sunstantially higher lattice and symmetry mismatch), the three-dimensional silicide nucleation still took place with a roughly equal probability on terraces as well as on the step-bunches.

It thus could be so far qualitatively concluded, that self-organization of the silicide nanostructure islands on the step-bunches of the vicinal Si(111) surfaces requires the deposition method to be solid-phase epitaxy (rather than reactive phase epitaxy), and the coverage to be low (most probably at a sub-monolayer level).

3. *Introduction*

Ever since its discovery in the early 90's [1-3], spontaneous formation (aka "self-assembly") and ordering (aka "self-organization") of nanometer size three-dimensional (3D) islands (hereby termed "nanocrystals") of perfect geometry and crystal structure on surfaces by heteroepitaxy (strained-layer growth on lattice-mismatched substrates) has been the focus of a great deal of research effort. Self-assembled quantum-well, -wire, and -dot nanostructures are not only interesting from a purely fundamental point of view. Their unique, atom-like electronic structure and properties [4] pave the way to bottom-up made LED's and lasers [5,6], single-electron transistors (SET's) [7,8] and logic gates based on charge or spin quantum cellular automata (QCA) [9,10]. In addition, improved catalytic reactions in the presence of metallic nanoparticles on surfaces have been reported [11,12]. Fabrication of such tiny nanometric devices by a conventional top-down approach is not easily achieved. So far, many efforts have been devoted to group-IV elemental [Si, Ge] (13-19) and II-VI & III-V compound semiconductor nanostructures (especially direct band-gap arsenides and antimonides) for photonic applications [4-6]. However, the ability of metal and metal-silicide nanostructures to self-assemble in a compact or elongated form [11,20-22], in conjunction with their room-temperature (RT) Coulomb-blockade and -staircase characteristics [23], makes them potential components in single electron devices. However, to use them in real devices requires control over the size, shape, and uniformity of the nanocrystals in the array, and for certain applications, such as QCA [9,10], spatial ordering into desired patterns as well.

Tersoff and co-workers have attributed the formation of isolated, shallow, strained heteroepitaxial nanocrystals to elastic relaxation due to the appearance of tilted facets, in spite of the respective excess facet energies [24,25]. This allowed them to establish fundamental relations between the nanocrystal size, shape and nucleation barrier, and the mismatch strain. Despite the apparent simplicity of the model, which neglected the effects of nanocrystal edges and corners as well as the nanocrystal-nanocrystal interactions and entropy, it has been recently quantitatively confirmed by a powerful combination of first-principles calculations and continuum modeling [26], as well as by convincing experimental results. For example, Goldfarb *et al.* have found pyramidal pits in Ge/Si(001) epilayers (predicted to relieve the strain even more effectively than the pyramidal nanocrystal themselves) to precede the nanocrystals [15], and by varying the composition, x , of a component in a binary system, Dorsch and co-workers have confirmed the size dependence on the square of strain for $\text{Si}_{1-x}\text{Ge}_x$ nanocrystals [27]. Brongersma and co-workers have also demonstrated equilibrium elongation of isolated CoSi_2 nanocrystals, obtained by Co-implantation and annealing, upon exceeding a certain critical size calculated according to Tersoff's model [28] (even though epitaxial CoSi_2

nanocrystals did not seem to exactly obey that model [29]). By explicitly including edge contributions, anisotropic surface stress and island-island interactions in the calculations, ordered patterns of 2D and 3D nanocrystals which are stable against ripening [30] have been predicted to form [4] and were experimentally observed [31]. In addition to equilibrium elongation [24,28], another interesting strain-induced phenomenon, namely a height-increasing (thickening) nanocrystal shape transition, has been found in both elemental Ge/Si(001) [16,18,19] and compound InAs/GaAs(001) [32]) semiconductor heterosystems, as well as in the transition metal-silicides [21,29]. Perhaps one of the most challenging issues in self-assembly and self-organization is the prevention of Ostwald ripening, where larger nanocrystals grow at the expense of smaller ones due to the Gibbs-Thomson effect [30,33]. The problem is that this process creates undesirably broad, negatively skewed nanocrystal size distributions [30]. Homoepitaxial islands are inherently unstable against Ostwald ripening, however heteroepitaxial ones may be stabilized by the difference in surface stress tensors between them and the substrate, which leads to force multipoles at the boundary between them and resistance to ripening even if the mismatch is very low [4]. If sufficiently high (at least a few percent) mismatch is present, the growth can be self-limiting because the barrier to adatom attachment to the growing nanocrystal due to the strained ribbon at the nanocrystal-substrate contact region [34] scales with the island size [35,36]. Either way, the size and separation distance of heteroepitaxial nanocrystals are determined by elastic interactions. Nanocrystals interact repulsively with each other through the substrate, and this strain-dependent repulsion controls the mean separation distance between them [37]. A better although more complex way not only to fix the nanocrystal size, but the mean separation distance and ordering, is by growing strained multilayered nanocrystal superlattices [38,39], where the nanocrystals interact both in-plane and out-of-plane with neighbors in adjacent layers. Consequently, vertically and spatially correlated nanocrystals can result [38,39]. Also in this case elastic interactions play a major role in defining the shape and distribution of the nanocrystals.

In this research, we investigate what appears to be an entirely different mechanism of nanocrystal size selection and ordering, where the major role is played by the localized kinetics of metal-silicon reaction at a stepped surface, rather than by elasticity. The observed phenomena can be divided into three major ones: (a) preferential decoration of vicinal step-bunches by nanocrystals, (b) size-selection of the step-bunch nanocrystals, and (c) ordered arrangement of these nanocrystals, with some mean periodic nanocrystal-nanocrystal separation along the parent step-bunch ledges. As can be expected from a simple terrace-ledge-kink (TLK), or terrace-step-kink (TSK), model [33], due to the increased coordination of the adatoms at the step-bunch sites, these are the preferred sites for adatoms (provided the adatoms are sufficiently mobile to cross terraces and reach the steps), which explains the preferential

decoration of step-bunches [40] by the CoSi_2 nanocrystals [41]. Using the same reasoning, Si atoms for the reaction on such a step-bunched surface should be almost exclusively supplied by the steps in bunches (“staircases” or “trains”, where Si atoms are less strongly bonded than at the terraces), which may account for the correlation between the size of the metal-silicide nanocrystals and the bunch height [42]. Another model, based on de-wetting and downhill migration of the islands across the step-edges, where island thickening is achieved without surmounting the associated nucleation barrier, has been proposed by Ling *et al.* [43] and McCarty [44]. Finally, the creation of mean periodicity between the step-bunch nanocrystals can be explained by mutual repulsion, based on the overlapping of either mismatched-strain fields [37] or, as has been recently put forward by Salac *et al.* [45,46] – contact potential charge clouds in the substrate.

4. Methods, Assumptions, and Procedures

Aims and Objectives

This research aims at establishing the complex relations between the surface properties of singular and vicinal Si surfaces, the metal deposition methods and parameters (as well as post-deposition thermal treatment regimes), and the resulting epitaxial nucleation, evolution and ordering of self-assembled metal-silicide nanostructures. While metals on Si and metal-silicon reactions are important for classical applications as contact and interconnect *continuous films* in VLSI and ULSI, this research is expected to advance the understanding of the interaction of metals with Si surfaces in a very different respect, namely in the form of variously shaped *isolated silicide islands* to be used as building nanocomponents in novel electronic and photonic devices, such as logic gates and QCA’s. The details of the Si surface (crystalline orientation, doping, miscut angle) determines its properties, directly affects interaction with the deposited metal adatoms, and in conjunction with the metal deposition method, determines the silicide formation kinetics and the properties of the silicide/silicon interface. Morphological and statistical characteristics, and the resulting collective and individual electronic properties of the so-formed 2D and/or 3D nanostructure (island) arrays, depend in a complex manner on these factors. While quite a few works on self-assembled silicides are documented in the literature, only a handful showed some evidence of self-ordering. The research in this field seems to be quite sporadic, and hence the purpose of this research is to conduct systematic, coherent studies with well-defined goals, aimed at a deeper understanding of this topic and, ultimately, at producing a generic model capable of predicting (and controlling) the self-organizational behavior of metal-silicide islands on silicon.

The objectives of the proposed research are:

(i) Development of procedures for the preparation of self-patterned Si templates for self-organizational silicide-nanostructure growth. These consist of high-temperature flashes of the vicinal Si(111) substrates in UHV, by passing direct current (both polarities) at different angles to the step-edges, for electro-migration assisted structurization. The resulting variously shaped and sized “step-terrace” surface structure and morphology are analyzed *in-situ* in reciprocal space by surface electron diffraction [low- (LEED) and reflection high- (RHEED) energy electron diffraction] and in real space by scanning probe microscopy methods [mainly by scanning tunneling microscopy (STM)]. The resulting surface morphological features from real space STM images will be analyzed to yield the mean statistical characteristics of the surface, such as terrace width and step-bunch height. This stage should amplify our capability to control the template periodicity (terrace width) and depth (step-bunch height), in addition to the values dictated by the miscut angle.

(ii) Self-organization of silicide nanostructures on the Si templates. Two pre-selected metals, Co and Ti, undergo evaporation onto self-patterned Si templates in a controlled manner using a precise e-beam evaporator. Due to the purpose-designed geometry of the UHV-STM chamber, where the e-beam evaporator is incident upon the sample mounted in the SPM stage, the metal-surface interaction in the course of deposition has been studied in *real time*. Two deposition methods have been utilized for this study: reactive deposition epitaxy (RDE), where the metal flux is incident upon a pre-heated substrate, and solid-phase epitaxy (SPE), where the metal is deposited at room temperature (RT) and subsequently annealed to promote silicide formation. The evaporator flux monitor will be independently calibrated to allow for the coverage estimation. The annealing treatments are conducted under a continuous surface imaging to detect every evolutionary change *as it happens*, and to fix (and, if required, quench) the surface condition for detailed diffraction and microscopic analyses. Applying bias dependent imaging in STM and scanning tunneling spectroscopy (STS) is expected to shed light on the chemistry and electronic structure of the silicide nanostructures. Again, the STM images will be computer analyzed to yield all the important statistical details of the nanostructure arrays, such as size distributions, neighbor statistics, coverage, azimuthal and radial correlations, shape and anisotropy, degree and direction of ordering, etc., using especially purchased for this purpose SPIP software by Image Metrology. Details of the silicide nanostructure formation and evolution will be correlated to the initial, pre-contact template morphology and deposition method and parameters.

Materials selection

The metals for the proposed studies, namely Co and Ti, have been selected to represent a difference in mismatches of their respective silicides to silicon and/or to show a tendency for ordering on the one hand, and to exhibit technologically important and potentially useful physical properties, on the other hand. TiSi_2 exhibits a very large lattice and symmetry mismatch to Si (anisotropic and hence depends on the direction in the coincidence lattice and the polymorph, i.e., C49- TiSi_2 or C54- TiSi_2), and yet its nanostructures bare many similarities to the low-mismatched ($\sim 1.2\%$) CoSi_2 [21,29,42,47], thus the comparison between them is supposed to, at least, single out the effect of mismatch strain. In addition, TiSi_2 nanostructures exhibit Coulomb-blockade and –staircase even at RT [23], and CoSi_2 shows a profound tendency for ordering [42,47] (see Fig. 1). Both silicides are widely used in VLSI.

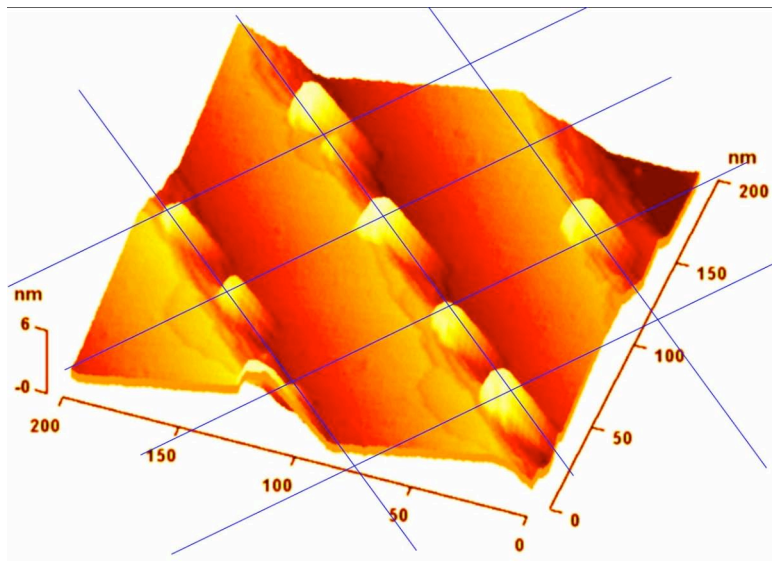


Figure 1: CoSi_2 nanocrystals self-ordered on the vicinal Si(111) step-bunches.

Methods

The nanostructure-synthesis and *in-situ* ultra-high vacuum (UHV) surface science characterization have been conducted in the “Surface Science and Nanostructures” laboratory at TAU, under the leadership of I. Goldfarb. The laboratory is centered around a multi-purpose variable-temperature UHV SPM (Omicron model AFM-25), which can be operated in STM and atomic force microscopy (AFM) modes, where metal evaporation, heat treatments, and subsequent analyses are carried-out. Usually, layer deposition and growth is monitored with

reflection high-energy electron diffraction (RHEED). One of the bigger advantages of this method is the ease of counting the deposited monolayers (ML's) from the specular beam oscillations. On the downside is the fact that, as with any indirect method, the interpretation of RHEED patterns without correlating them to real-space images is ambiguous and can lead to dubious conclusions. In this research, RHEED has been used for post-evaporation crystallographic and morphological analyses of the silicide nanostructure arrays with cross-referencing to the real-space SPM data. Metal deposition is performed from a three-pocket mini e-beam evaporator, capable of fully- or semi-automated operation and purpose-designed to incident upon the specimen mounted in the SPM stage. The growth monitoring is mostly performed by acquiring SPM images in real-time, at desired temperatures and under exposure to the metal fluxes. Such a *modus operandi* allows direct insight into the kinetics of processes, such as nucleation and growth, phase transitions at the surface, and metal-semiconductor reactions, as they happen and with high resolution. For example, this method has allowed the author to observe gas-source molecular beam epitaxial (GS-MBE) growth of Si and Ge layers [13,48-50] and, what is more relevant to this proposal, metal (Co, Ti) reactions with Si and Ge surfaces [20,21,29,42,47,51-56] from the very initial stages of very low coverage adsorption of metal particles, where site-specific as well as random nucleation could be studied in detail, to the final stages of evolution of the fully grown nanocrystals. Fig. 2 illustrates the power of such an approach on the example of the initial stages of epitaxial CoSi_2 growth by solid-phase epitaxy (SPE, at RT+anneals) of Co on a Si(111) surface, where adsorption of the initial tiny sub-monolayer Co agglomerates in the form of white blobs (on the right) is observed in detail at the initially bare and ideal Si(111)-(7 \times 7) surface (on the left).

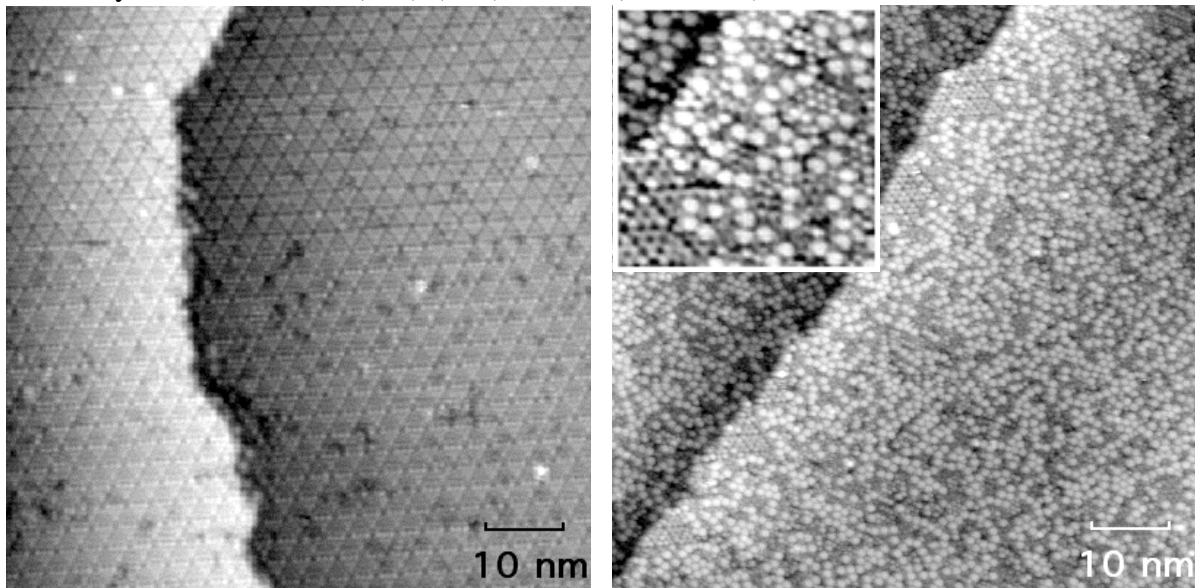


Figure 2: Co/Si(111)-(7 \times 7) nucleation.

When the STM mode is chosen to monitor the growth, the current-voltage (I - V) spectra can be obtained from the evolving features with a highest spatial resolution, using scanning tunneling spectroscopy (STS), so that not only the morphology and crystal structure of the evolving nanostructures can be studied, but their electronic structure, as well.

Additional analytical tools integrated within the UHV microlab for the subsequent *in-situ* investigations, are the low-energy electron diffraction (LEED) and Auger electron spectroscopy (AES), acquired by accordingly reconfiguring the same 4-grid analyzer, to obtain either LEED patterns or Auger electron spectra. The former are important for averaging the crystallographic surface analysis over larger areas, having the advantage on RHEED by instantly providing a 2D map of the reciprocal space, but suffering from lower sensitivity to the surface roughness. The latter, i.e. AES is important for deducing the cleanliness and the chemical composition of a surface under investigation, even though it is not suited for obtaining chemical composition of individual nanocrystals.

The combination of atomic-resolution real-space techniques, such as SPM, with the additional above mentioned surface science techniques, even if indirect, is a powerful one, which proves very effective in the author's past work. Constant-current and constant-height STM imaging at growth temperatures provides real-space sample topography with atomic resolution, voltage-dependent STM imaging contains information about surface electronic structure, and STS is directly linked to the local density of electronic surface states. However, electronic properties are best measured at low temperatures, to avoid thermal excitation. In addition, in some processes surface diffusion is so rapid, that even at RT the rates are too fast relative to the tip scanning speed. This demonstrates the need for cooling, and indeed cooling to less than 25 K is available, as well as heating up to 1400 K (1000 K in the SPM). Surface diffraction techniques, such as RHEED, provide important structural information averaged from areas larger than the normal STM's field of view. Such information is complementary to that obtained with an STM, and good structural analysis should be based on combination of real-space technique (STM/AFM) and reciprocal-space technique (RHEED/LEED). Additional peripheral equipment includes a residual gas analyzer (quadrupole spectrometer) to detect gaseous components in UHV and an ion-sputter gun for surface cleaning.

Such a set-up, based on real-time observation of surface evolution with SPM, and allowing working at both low and elevated temperatures, aided by all the complementary analytical tools described above, is quite unique, and thus the benefits arising from a research based on this state-of-the-art microlab shall be numerous. Most importantly, it will allow exploration of important processes, namely nanostructure self-assembly and their self-organizational tendencies from atomistic to nanometer level with utmost resolution *as they happen in real space and time!*

5. Results and Discussion

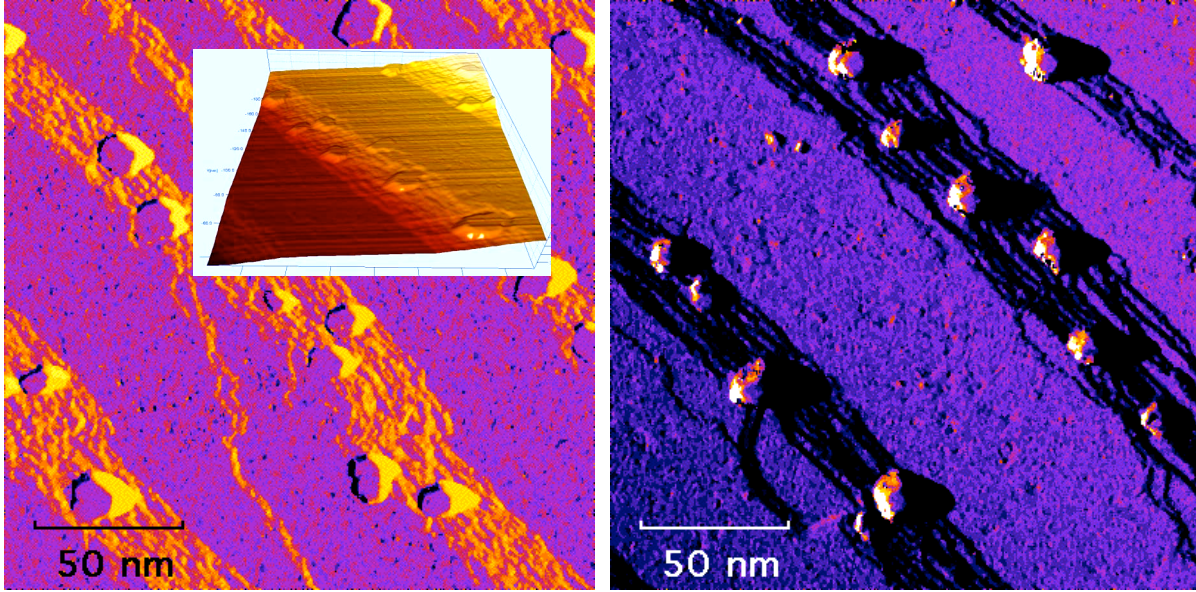


Figure 3: Formation of the precursor 2D CoSi_2 nanoplatelets (left), preceding the formation of fully grown 3D rounded nanocrystals self-ordered on the vicinal $\text{Si}(111)$ step-bunches (right).

The nanocrystal evolution can be observed in real time, upon annealing at elevated temperatures, as has been done for the case of the Co on vicinal $\text{Si}(111)$, where 2D platelets were first formed by growing mostly out of the individual steps in the bunch [left-hand side of Fig. 3 and the inset], with the subsequent platelet thickening to eventually form rounded 3D CoSi_2 nanocrystals self-ordered along the step-bunches [right-hand side of Fig. 3]. Real-time STM at elevated temperatures has allowed us to detect and analyze how such preferential self-organization takes place. Fig. 4(a) shows the process of Ostwald ripening of the step-bunch nanocrystals at the expense of the terrace-nanocrystals, and Fig. 4(b) shows the process of coalescence between the step-bunch nanocrystals. It turned out that only those residing at the step-bunches survived the ripening by an apparent stabilization by the parent step-bunches, which hence determined the nanocrystal size to be comparable with the bunch height. These relations between the parent bunch height and the nanocrystal size are especially clear when inspecting locally less ordered regions (deviating from the mean vicinality) with lower than the miscut-determined mean step-bunch height, which always exist on the sample's surface, where smaller nanocrystals occupy lower bunches [Fig. 4(c),(d)]. In addition, we have also found that there was a mean size-dependent periodicity along the step-bunches, i.e. 1D ordering, and locally, where the terrace width was compatible with the inter-cluster separation period along the bunch – 2D ordering, such as shown in Fig. 1 [42]. On the other hand, reactive deposition epitaxy (RDE, on the preheated substrates) of Co on the same $\text{Si}(111)$ did not result in such

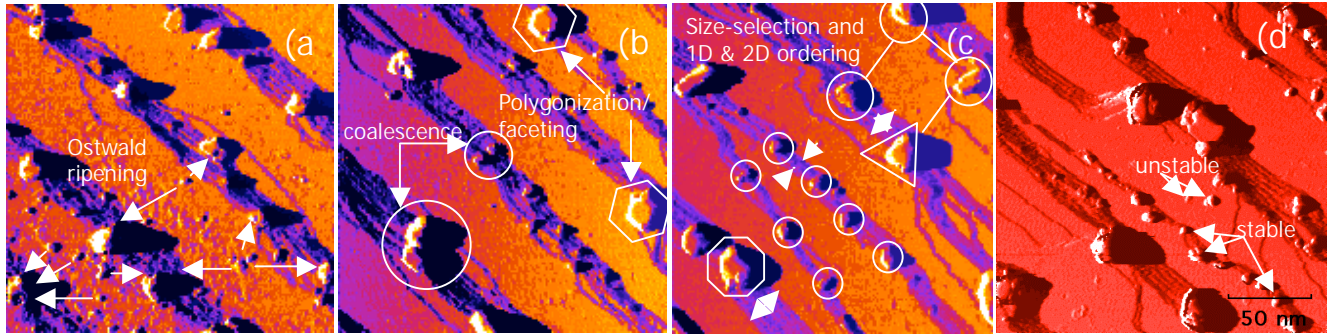


Figure 4: Self-organization of the SPE-grown CoSi_2 nanocrystals by stabilization at the vicinal Si(111) step-bunches.

ordering: while step-bunch nucleation (Fig. 5) was more dominant, non-negligible terrace nucleation (Fig. 5, on the right) was present as well [47]. However, the mere fact of using SPE is, apparently, insufficient by itself to guaranty self-organization: higher initial Co coverage did not result in ordering of CoSi_2 nanocrystals on the step-bunches either (Fig. 6), leading us to assume coverage dependence (this is one of the working hypotheses that will be targeted in the proposed research). It is also noteworthy, that the so-formed silicide islands are two-dimensional (2D), which grow in a fractal fashion by ripening and coalescence processes in an apparent attempt to cover the entire surface with as larger islands as possible. Small, 3D nanocrystals are observed at the step-bunches, perhaps even ordered to some degree in a quasi-hexagonal manner (e.g., see 470°C annealed surface in Fig. 6), however seem less dominant.

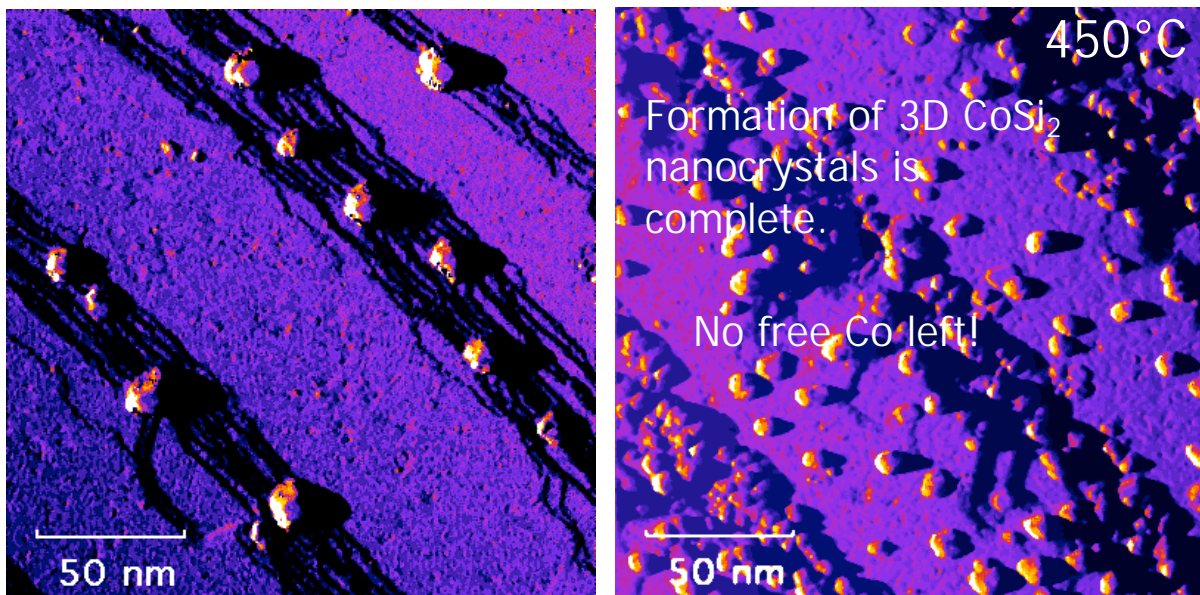


Figure 5: SPE-grown CoSi_2 nanocrystals self-ordered on the vicinal Si(111) step-bunches (left), to compare with disordered RDE-grown CoSi_2 nanocrystals on the same vicinal Si(111) surface (right).

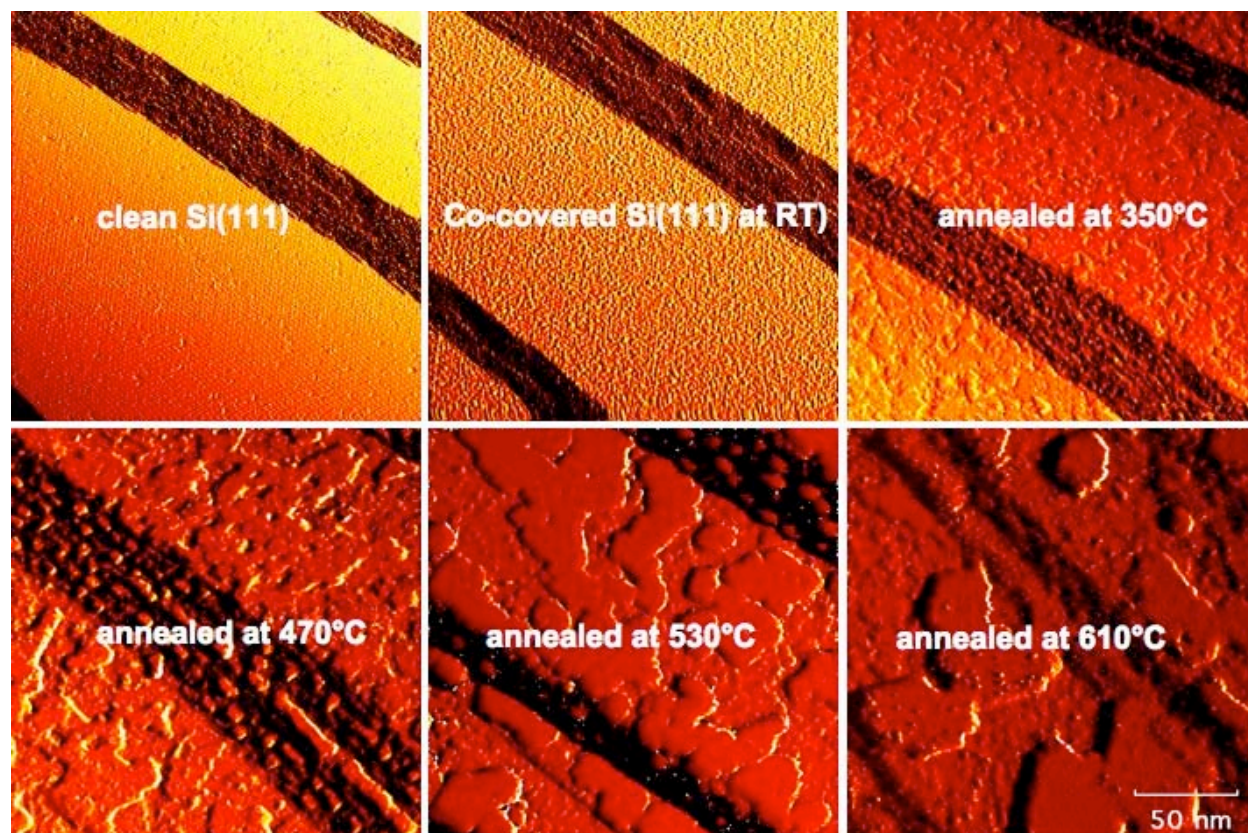


Figure 6: Evolution of the SPE-grown Co/Si(111) surface with annealing temperature. Formation and fractal growth of 2D silicide islands is evident.

The hypothesis of coverage dependence was also tested on the $\text{TiSi}_2/\text{Si}(111)$ nanocrystals. To isolate the higher-coverage effect from the influence of the deposition method, the nanocrystals were SPE grown. The results, shown in Fig. 7, are self-evident – in this case too, both terrace- and step-bunch nucleation and evolution of the silicide nanocrystals took place, resulting in a disordered appearance, shown in the figure. However, in this case the shape of the nanocrystal islands was still three-dimensional! This persistent 3D shape of the TiSi_2 nanocrystals, independent of the deposition method or the amount of the initial coverage, most probably originates at a very high lattice and symmetry mismatch between the TiSi_2 and the Si substrate. It is interesting to note, that this is not the case for the $\text{CoSi}_2/\text{Si}(111)$ epitaxial islands. When RDE and low-coverage SPE are used, the shape of the epitaxial CoSi_2 nanocrystals is 3D, very similar to that of the TiSi_2 ones. However, at higher coverages the shape of the nanoislands is clearly 2D, as shown in Fig. 6, implying that growth and phase-formation kinetics in this case play a more important role than the nominally very low lattice mismatch with Si ($\sim 1.2\%$), especially bearing in mind that there is no symmetry mismatch between the fluorite CoSi_2 crystal structure and the diamond Si one!

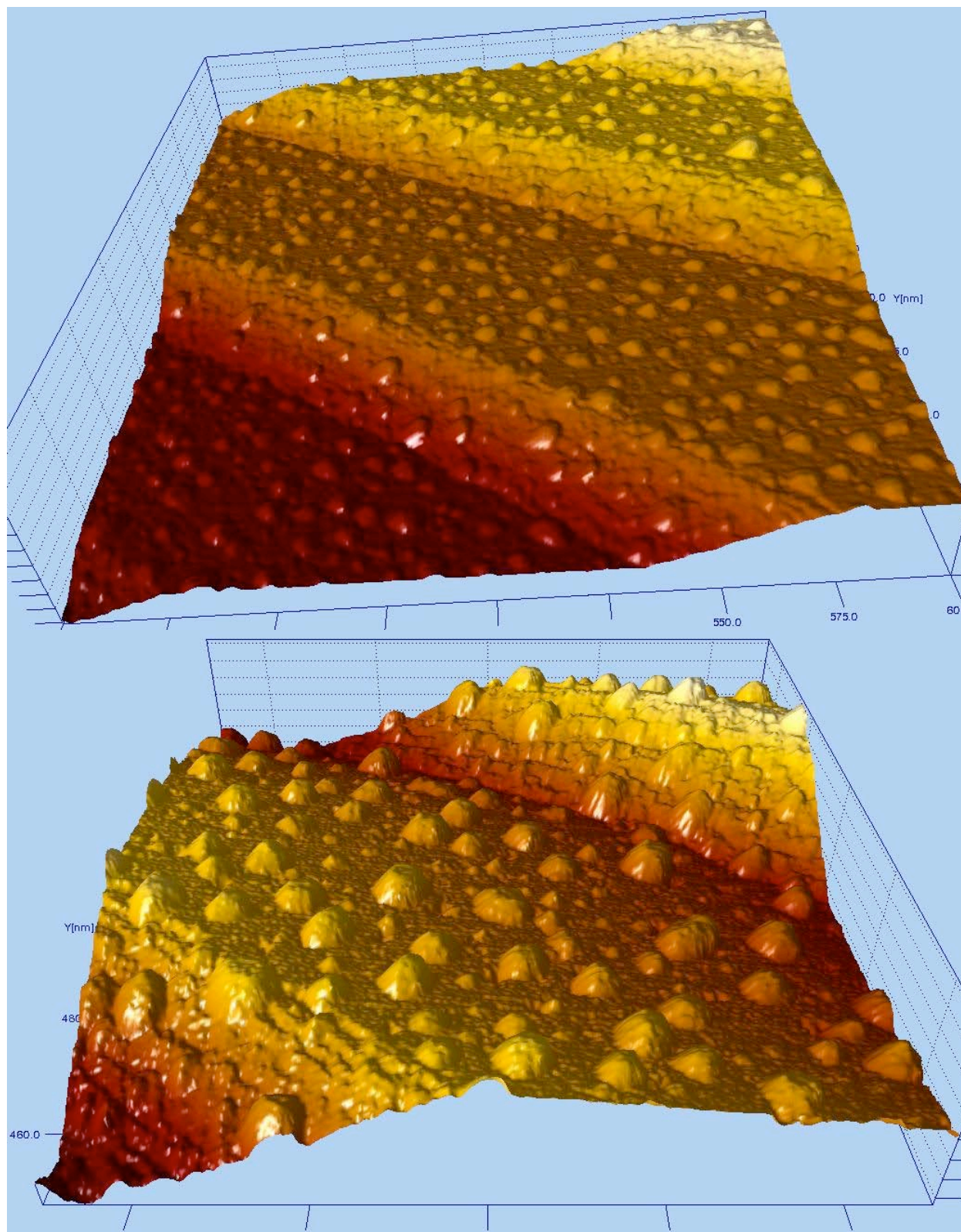


Figure 7: Lower (top) and higher (bottom) STM magnification of disordered TiSi_2 nanocrystals, SPE-grown on a vicinal Si(111) surface with higher Ti coverage.

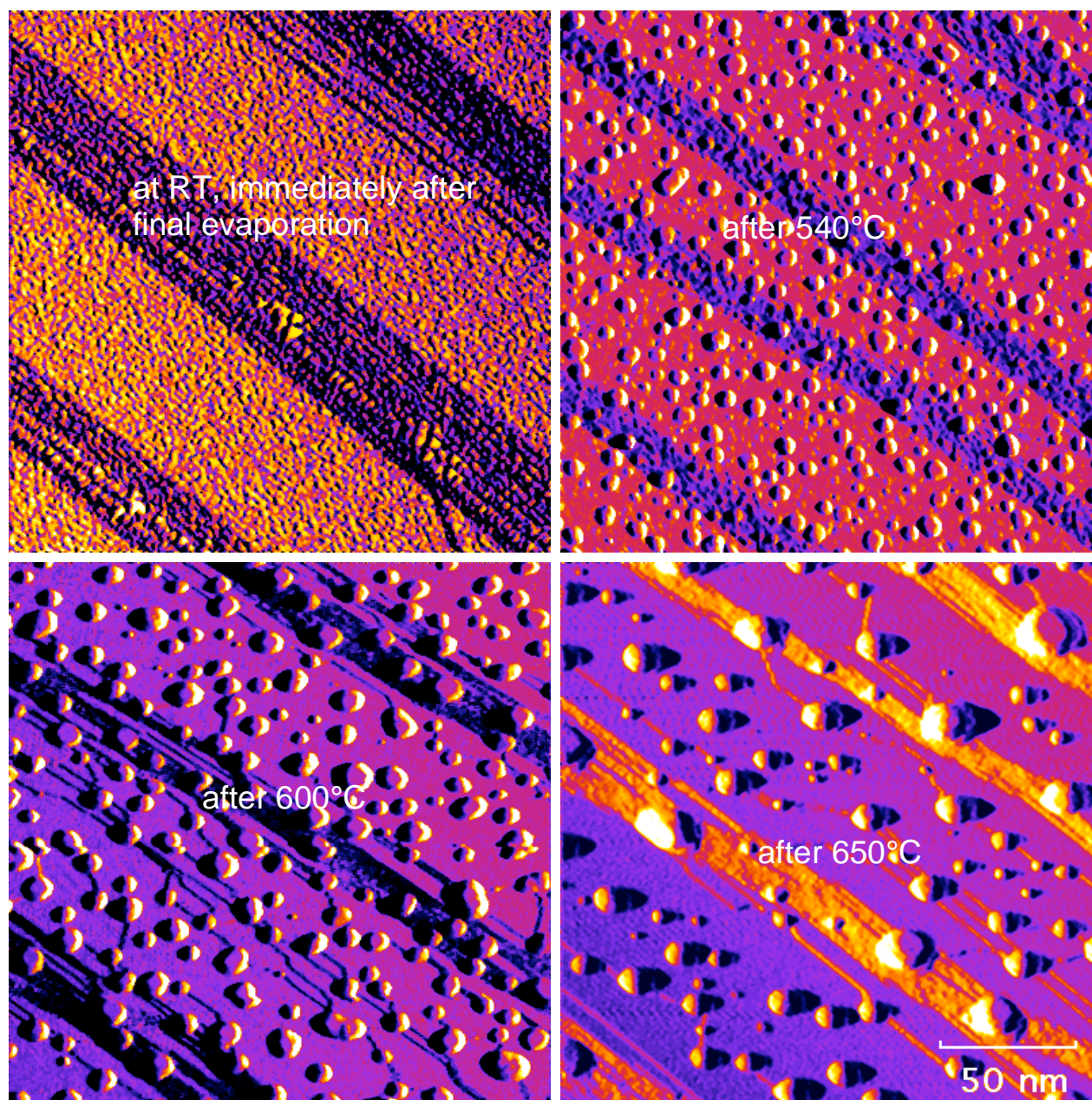


Figure 8: Evolution of the SPE- TiSi_2 nanocrystals, grown on a vicinal $\text{Si}(111)$ surface with higher Ti coverage, as a function of annealing temperature.

Closer examination of the evolution of the $\text{TiSi}_2/\text{Si}(111)$ nanocrystals in Fig. 8 reveals, that the late-stage growth mode is governed predominantly Ostwald ripening, as can be easily judged by (i) broadening of the size distribution, and (ii) increasing mean size with (iii) simultaneously decreasing coverage. Thus, there is no size selection mechanism similar to the low-coverage $\text{CoSi}_2/\text{Si}(111)$, as shown in Figs. 3, 4, 5(a), and, especially 1, even though many

of the TiSi_2 nanocrystals after 650°C anneal [Fig. 8(d)] occupy step- and step-bunch edges. It appears [cf. Fig. 8(d)], that while annealing the SPE-grown TiSi_2 nanocrystals tends to cause certain degree of their preferential occupation of the step-bunches, neither the occupation is perfect (many are still found at the midst of terraces), nor the size-selection mechanism is in effect (no relation between the nanocrystal sizes and the parent step- or step-bunch height).

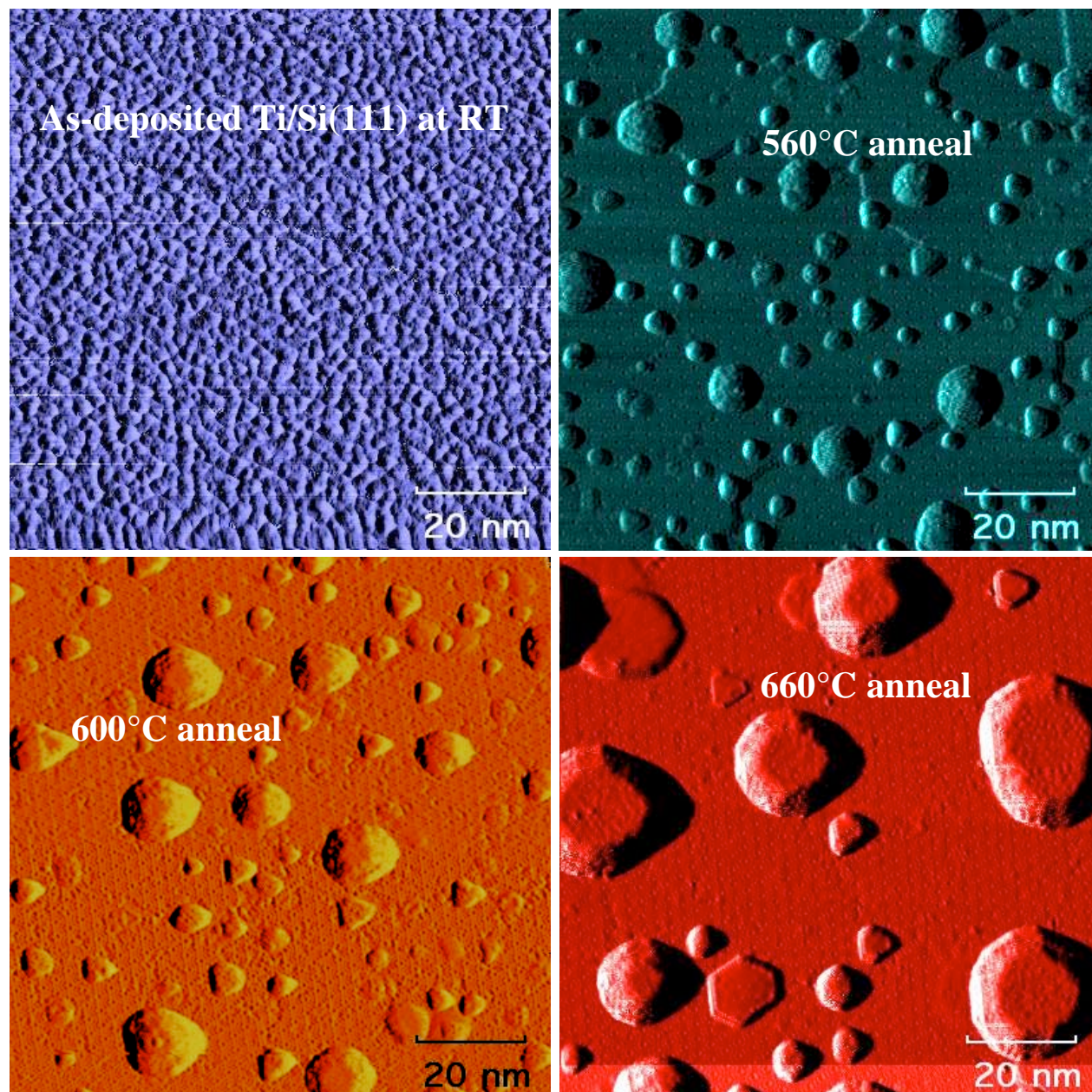


Figure 9: Evolution of the SPE- TiSi_2 nanocrystals, grown on a *singular* Si(111) surface, as a function of annealing temperature.

Finally, to elucidate the effect of the substrate step structure and morphology, similar coverage of Ti and Co, respectively, was SPE-deposited on singular Si(111) substrates, subsequently undergoing identical annealing cycles. Fig. 9 shows the evolution of the TiSi_2 nanocrystals, and Fig. 10 shows the finite state of the CoSi_2 ones.

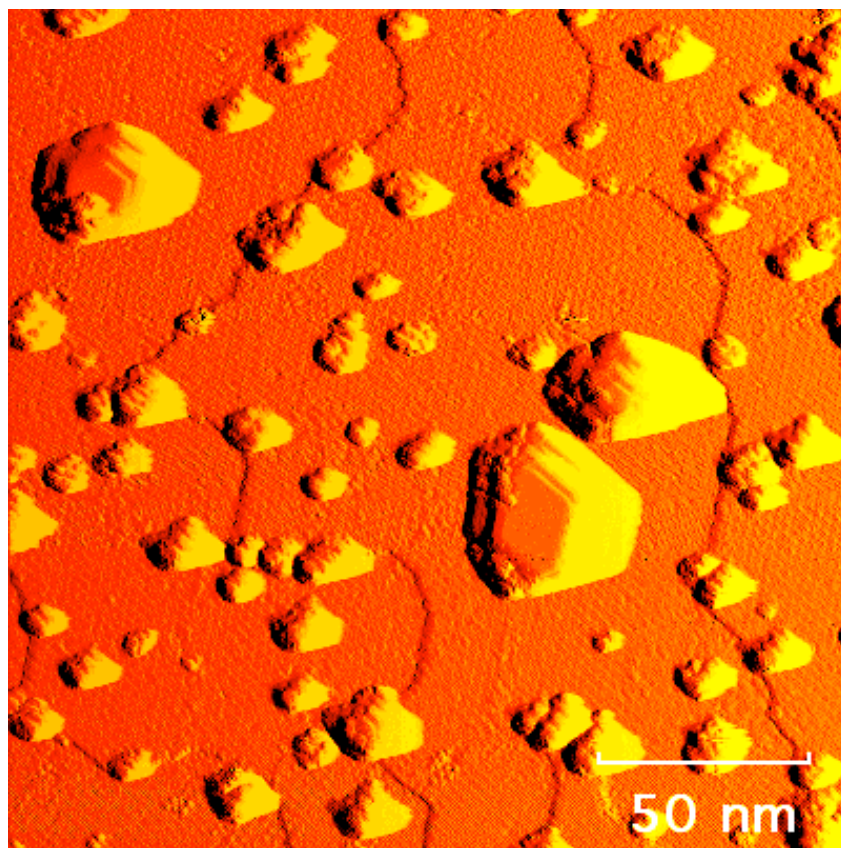


Figure 10: SPE- CoSi_2 nanocrystals, grown on a *singular* Si(111) surface, after a 650°C annealing.

6. *Conclusions*

This research aims at establishing the complex relations between the surface properties of singular and vicinal Si surfaces, the type of metal, metal deposition methods and parameters (as well as post-deposition thermal treatment regimes), and the resulting epitaxial nucleation, evolution and ordering of self-assembled metal-silicide nanostructures.

The main conclusions that so far stem from the research emphasize the importance of the metal type, deposition method, and of the initial metal coverage. More specifically, the results (for both CoSi_2 and TiSi_2) imply a better suitability of the solid-phase epitaxy (SPE) than that of reactive deposition epitaxy (RDE) for self-organization of the silicide nanocrystals on the step-

bunch ledges of the vicinal Si(111) surfaces. The results also imply that low, probably sub-monolayer, coverages are required to produce that effect of self-ordering at the step-bunches. However, the degree of self-ordering was substantially higher in the case of CoSi₂ nanocrystals than in the TiSi₂ ones, let alone the size-selection, that was reasonably good in CoSi₂, but practically non-existent in the TiSi₂ case.

Even though some sort of ordering of small three-dimensional cobalt silicide nanocrystals took place upon SPE of higher Co coverage on vicinal Si(111), at the same time large fractal two-dimensional silicide islands covered major portion of the terraces. In case of Ti/Si(111) SPE at a similar coverage, again the nanoislands were formed at the both step-bunch ledges and terraces, however at both type of sites they assumed identical three-dimensional shape of truncated cones, with no visible correlation between them and their parent step- and step-bunch heights.

Finally, no self-ordering or size-selection of any sort was found in both the CoSi₂ and the TiSi₂ nanocrystals, when grown (even using SPE) on singular Si(111) surfaces. As expected, periodic step-bunch – terrace – step-bunch substrate structure is imperative for any type of ordering. Even heteroepitaxial system with clearly pronounced ordering tendencies, such as CoSi₂/Si(111) nanocrystals [(let alone TiSi₂/Si(111))], does not self-organize in the absence of such periodic substrate structure.

A paper on the subject is in preparation these days, and will, of course, include an appropriate acknowledgement of the funding agency, as will all the subsequent papers that may stem from this funded period.

7. References

1. D. J. Eaglesham and M. Cerullo, “*Dislocation-free Stranski-Krastanow growth of Ge on Si(100)*”, Phys. Rev. Lett. **64**, 1943 (1990).
2. Y.-W. Mo, D. E. Savage, B. S. Swartzentruber, M. G. Lagally, “*Kinetic pathway in Stranski-Krastanov growth of Ge on Si(001)*”, Phys. Rev. Lett. **65**, 1020 (1990).
3. S. Guha, A. Madhukar, K. C. Rajkumar, “*Onset of incoherency and defect introduction in the initial stages of molecular-beam epitaxial growth of highly strained In_xGa_{1-x}As on GaAs(100)*”, Appl. Phys. Lett. **57**, 2110 (1990).
4. V. A. Schukin, N. N. Ledentsov, D. Bimberg, *Epitaxy of Nanostructures* (Springer-Verlag, Berlin Heidelberg, 2004).
5. C. B. Murray, C. R. Kagan, M. G. Bawendi, “*Self-organization of CdSe nanocrystallites into 3-dimensional quantum-dot superlattices*”, Science **270**, 1335 (1995).

6. S. Fafard, K. Hinzer, S. Raymond, M. Dion, J. McCaffrey, Y. Feng, S. Charbonneau, “*Red-emitting semiconductor quantum-dot lasers*”, *Science* **274**, 1350 (1996).
7. A. P. Alivisatos, “*Electrical studies of semiconductor-nanocrystal colloids*”, *MRS Bull.* **23**(2), 19 (1998).
8. J. Repp, G. Meyer, F. E. Olsson, M. Persson, “*Controlling the charge state of individual gold adatoms*”, *Science* **305**, 493 (2004).
9. A. Orlov, I. Amlani, G. H. Bernstein, C. S. Lent, G. L. Snider, “*Realization of a functional cell for quantum-dot cellular automata*”, *Science* **277**, 928 (1997).
10. A. Imre, G. Csaba, L. Ji, A. Orlov, G. H. Bernstein, V. Metlushko, W. Porod, “*Majority logic gate for magnetic quantum-dot cellular automata*”, *Science* **311**, 205 (2006).
11. M. Valden, X. Lai, D. W. Goodman, “*Onset of catalytic activity of gold clusters on titania with the appearance of nonmetallic properties*”, *Science* **281**, 1647 (1998).
12. J. V. Lauritsen, M. Nyberg, J. K. Nørskov, B. S. Clausen, H. Topsøe, E. Lægsgaard, F. Besenbacher, “*Hydrodesulfurization reaction pathways on MoS₂ nanoclusters revealed by scanning tunneling microscopy*”, *J. Catal.* **224**, 94 (2004).
13. I. Goldfarb, J.H.G. Owen, P.T. Hayden, D.R. Bowler, K. Miki, and G.A.D. Briggs, “*Gas-source growth of group IV semiconductors: III. Nucleation and growth of Ge/Si(001)*”, *Surf. Sci.* **394**, 105 (1997).
14. I. Goldfarb, P.T. Hayden, J.H.G. Owen, and G.A.D. Briggs, “*Competing growth mechanisms of Ge/Si(001) coherent clusters*”, *Phys. Rev. B.* **56**, 10459 (1997).
15. I. Goldfarb, P.T. Hayden, J.H.G. Owen, and G.A.D. Briggs, “*Nucleation of “hut” pits and clusters during gas-source molecular beam epitaxy of Ge/Si(001) in in-situ scanning tunneling microscopy*”, *Phys. Rev. Lett.* **78**, 3959 (1997).
16. I. Goldfarb, “*Effect of strain on the appearance of subcritical nuclei of Ge nanohuts on Si(001)*”, *Phys. Rev. Lett.* **95**, 025501 (2005).
17. I. Goldfarb, L. Banks-Sills, R. Eliasi, “*Is the elongation of Ge huts in the low-temperature regime governed by kinetics?*”, *Phys. Rev. Lett.* **97**, 206101 (2006).
18. G. Medeiros-Ribeiro, A. M. Bratkovski, T. I. Kamins, D. A. A. Ohlberg, R.S. Williams, “*Shape transition of Ge nanocrystals on a Si(001) surface from pyramids to domes*”, *Science* **279**, 353 (1998).
19. F. M. Ross, R. M. Tromp, M. C. Reuter, “*Transition states between pyramids and domes during Ge/Si island growth*”, *Science* **286**, 1931 (1999).
20. I. Goldfarb and G. A. D. Briggs, “*Reactive deposition epitaxy of CoSi₂ nanostructures on Si(001): nucleation and growth and evolution of dots during anneal*”, *Phys. Rev. B* **60**, 4800 (1999).

21. I. Goldfarb, G. Cohen-Taguri, S. Grossman, M. Levinshtein, “*Equilibrium shape of titanium silicide nanocrystals on Si(111)*”, Phys. Rev. B **72**, 075430 (2005).
22. Y. Chen, D. A. A. Ohlberg, R. S. Williams, “*Nanowires of four epitaxial hexagonal silicides grown on Si(001)*”, J. Appl. Phys. **91**, 3213 (2002).
23. J. Oh, V. Meunier, H. Ham, R. J. Nemanich, “*Single electron tunneling of nanoscale $TiSi_2$ islands on Si*”, J. Appl. Phys. **92**, 3332 (2002).
24. J. Tersoff and R. M. Tromp, “*Shape transition in growth of strained islands – spontaneous formation of quantum wires*”, Phys. Rev. Lett. **70**, 2782 (1993).
25. J. Tersoff and F. K. LeGoues, “*Competing relaxation mechanism in strained layers*”, Phys. Rev. Lett. **72**, 3570 (1994).
26. Q.-H. Lu and F. Liu, “*Towards quantitative understanding of formation and stability of Ge hut islands on Si(001)*”, Phys. Rev. Lett. **94**, 176103 (2005).
27. W. Dorsch, H. P. Strunk, H. Wawra, G. Wagner, J. Groenen, R. Carles, “*Strain-induced island scaling during $Si_{1-x}Ge_x$ heteroepitaxy*”, Appl. Phys. Lett. **72**, 179 (1998).
28. H. Brongersma, M. R. Castell, D. D. Perovic, M. Zinke-Allmang, “*Stress-induced shape transition of $CoSi_2$ clusters on Si(100)*”, Phys. Rev. Lett. **80**, 3795 (1998).
29. I. Goldfarb, “*In-plane and out-of-plane shape transitions of heteroepitaxially self-assembled nanostructures*”, Surf. Sci. **601**, 2756 (2007).
30. M. Zinke-Allmang, L. C. Feldman, M. H. Grabow, “*Clustering on surfaces*”, Surf. Sci. Rep. **16**, 381 (1992).
31. J. B. Hannon, J. Tersoff, R. M. Tromp, “*Surface stress and thermodynamic nanoscale size selection*”, Science **295**, 299 (2002).
32. G. Costantini, A. Rastelli, C. Manzano, R. Songmuang, O.G. Schmidt, K. Kern, H. v. Kanel, “*Universal shapes of self-organized semiconductor quantum dots: striking similarities between $InAs/GaAs(001)$ and $Ge/Si(001)$* ”, Appl. Phys. Lett. **85**, 5673 (2004).
33. Z. Zhang and M. G. Lagally, “*Atomistic processes in the early stages of thin-film growth*”, Science **276**, 377 (1997).
34. O. E. Shklyae, M. J. Beck, M. Asta, M. J. Miksis, P. W. Voorhees, “*Role of strain-dependent surface energies in $Ge/Si(001)$ island formation*”, Phys. Rev. Lett. **94**, 176102 (2005).
35. D. E. Jesson, K. M. Chen, S. J. Pennycook, “*Kinetic pathways to strain relaxation in the $Si-Ge$ system*”, MRS Bull. **21**(4), 31 (1996).
36. D. E. Jesson, G. Chen, K. M. Chen, S. J. Pennycook, “*Self-limiting growth of strained faceted islands*”, Phys. Rev. Lett. **80**, 5156 (1998).
37. H. T. Johnson and L. B. Freund, “*Mechanics of coherent and dislocated island morphologies in strained epitaxial material system*”, J. Appl. Phys. **81**, 6081 (1997).

38. J. Tersoff, C. Teichert, M. G. Lagally, “*Self-organization in growth of quantum dot superlattices*”, Phys. Rev. Lett. **76**, 1675 (1996).
39. G. Springholz, V. Holy, M. Pinczolits, G. Bauer, “*Self-organized growth of three-dimensional quantum-dot crystals with fcc-like stacking and tunable lattice constant*”, Science **282**, 734 (1998).
40. A. Sgarlata, P. D. Szkutnik, A. Balzarotti, N. Motta, F. Rosei, “*Self-ordering of Ge islands on step-bunched Si(111) surface*”, Appl. Phys. Lett. **83**, 4002 (2003).
41. M. A. Zilani, H. Xu, X.-S. Wang, A. T. S. Wee, “*Terrace width dependence of cobalt silicide nucleation on Si(111)-(7×7)*”, Appl. Phys. Lett. **88**, 023121 (2006).
42. I. Goldfarb, “*Step-mediated size-selection and ordering of heteroepitaxial nanocrystals*”, Nanotechnology **18**, 335304 (2007).
43. W. L. Ling, T. Giessel, K. Thurmer, R. Q. Hwang, N. C. Bartelt, K. F. McCarty, “*Critical role of substrate steps in de-wetting of crystalline thin films*”, Surf. Sci. **570**, L297 (2004).
44. K. F. McCarty, “*Deterministic positioning of three-dimensional structures on a substrate by film growth*”, Nano Letters **6**, 858 (2006).
45. D. Salac and W. Lu, “*Ordering of metallic quantum dots*”, Appl. Phys. Lett. **89**, 073105 (2006).
46. W. Lu and D. Salac, “*Interaction of metallic quantum dots on a semiconductor substrate*”, Phys. Rev. B **74**, 073304 (2006).
47. I. Goldfarb and M. Levinshtein, “*Self-organization of cobalt-silicide nanoislands on stepped Si(111) as a function of growth method*”, J. Nanosci. Nanotechnol. **8**, 801 (2008).
48. J.H.G. Owen, K. Miki, D.R. Bowler, C.M. Goringe, I. Goldfarb, and G.A.D. Briggs, “*Gas-source growth of group IV semiconductors: I. Si(001) nucleation mechanisms*”, Surf. Sci. **394**, 79 (1997).
49. J.H.G. Owen, K. Miki, D.R. Bowler, C.M. Goringe, I. Goldfarb, and G.A.D. Briggs, “*Gas-source growth of group IV semiconductors: II. Growth regimes and the effect of hydrogen*”, Surf. Sci. **394**, 91 (1997).
50. I. Goldfarb, J.H.G. Owen, D.R. Bowler, C.M. Goringe, P.T. Hayden, K. Miki, D.G. Peettifor, and G.A.D. Briggs, “*In situ observation of gas-source molecular beam epitaxy of Si and Ge on Si(001)*”, J. Vac. Sci. Technol. **A16**, 1938 (1998).
51. I. Goldfarb and G.A.D. Briggs, “*Self-assembled metal-semiconductor compound nanocrystals on group IV semiconductor surfaces*”, Surf. Sci. **454-456**, 837 (2000).
52. I. Goldfarb and G.A.D. Briggs, “*Surface studies of phase formation in Co-Ge system: reactive deposition epitaxy versus solid phase epitaxy*”, J. Mater. Res. **16**, 744 (2001).

53. I. Goldfarb and G.A.D. Briggs, *Analysis of complex heterogeneous surfaces by bias-dependent scanning tunneling microscopy and spectroscopy*, Mater. Sci. Eng. B **91-92**, 115 (2002).
54. I. Goldfarb and G.A.D. Briggs, *Morphological evolution of epitaxial cobalt-semiconductor compound layers during growth in a scanning tunneling microscope*, J. Vac. Sci. Technol. B **20**, 1419 (2002).
55. I. Goldfarb, S. Grossman, G. Cohen-Taguri, and M. Levinshtein, *Scanning tunneling microscopy of titanium silicide nanoislands*, Appl. Surf. Sci. **238**, 29 (2004).
56. I. Goldfarb, S. Grossman, G. Cohen-Taguri, *Evolution of epitaxial titanium silicide nanocrystals as a function of growth method and annealing treatments*, Appl. Surf. Sci. **252**, 5355 (2006).

8. *List of Symbols, Abbreviations, and Acronyms*

| | | |
|--------|---|---|
| 2D | – | two-dimensional |
| 3D | – | three-dimensional |
| LED | – | light emitting diode |
| SET | – | single electron transistor |
| QCA | – | quantum-dot cellular automata |
| RT | – | room temperature |
| TLK | – | terrace-ledge-kink |
| TSK | – | terrace-step-kink |
| VLSI | – | very large scale integration |
| ULSI | – | ultra large scale integration |
| LEED | – | low-energy electron diffraction |
| RHEED | – | reflection high-energy electron diffraction |
| SPM | – | scanning probe microscopy |
| STM | – | scanning tunneling microscopy |
| STS | – | scanning tunneling spectroscopy |
| AFM | – | atomic force microscopy |
| UHV | – | ultra-high vacuum |
| AES | – | Auger electron spectroscopy |
| ML | – | monolayer |
| MBE | – | molecular beam epitaxy |
| GS-MBE | – | gas-source molecular beam epitaxy |